1989 NASA/ASEE SUMMER FACULTY FELLOWSHIP PROGRAM

JOHN F. KENNEDY SPACE CENTER
UNIVERSITY OF CENTRAL FLORIDA

STUDY OF METAL CORROSION USING AC IMPEDANCE TECHNIQUES IN THE STS LAUNCH ENVIRONMENT

PREPARED BY:	Dr. Luz M. Calle
ACADEMIC RANK:	Associate Professor
UNIVERSITY AND DEPARTMENT:	Randolph-Macon Woman's College Chemistry Department
NASA/KSC	
DIVISION:	Materials Science Laboratory
BRANCH:	Materials Testing Branch
NASA COLLEAGUE:	Mr. Louis G. MacDowell III
DATE:	August 11, 1989
CONTRACT NUMBER:	University of Central Florida NASA-NGT-60002 Supplement: 2

ACKNOWLEDGEMENT

I would like to thank my NASA colleague, Louis G. MacDowell, III, for providing me with the opportunity and orientation to pursue this research. I would also like to thank the people in the Materials Science Laboratory who made me feel welcome at the Kennedy Space Center. I am grateful to NASA/ASEE for my selection as a faculty fellow in the 1989 NASA/ASEE program at the Kennedy Space Center. The expertise and kindness of the program director, Dr. E. Ramon Hosler, is also gladly acknowledged.

ABSTRACT

AC impedance measurements were performed to investigate the corrosion resistance of 19 alloys under conditions similar to the STS launch environment. The alloys were: Zirconium 702, Hastelloy C-22, Inconel 625, Hastelloy C-276, Hastelloy C-4, Inconel 600, 7Mo + N, Ferralium 255, Inco Alloy G-3, 20Cb-3, SS 904L, Inconel 825, SS 304LN, SS 316L, SS 317L, ES 2205, SS 304L, Hastelloy B-2, and Monel 400. AC impedance data were gathered for each alloy after one hour immersion time in each of the following three electrolyte solutions: 3.55% NaCl, 3.55% NaCl-0.1N HCl, and 3.55% NaCl-1.0N HCl. The data were analyzed qualitatively using the Nyquist plot and quantitatively using the Bode plot. Polarization resistance, Rp, values were obtained using the Bode plot. Zirconium 702 was the most corrosion resistant alloy in the three electrolytes. The ordering of the other alloys according to their resistance to corrosion varied as the concentration of hydrochloric acid in the electrolyte increased. The corrosion resistance of Zirconium 702 and Ferralium 255 increased as the concentration of hydrochloric acid in the electrolyte increased. The corrosion resistance of the other 17 alloys decreased as the concentration of the hydrochloric acid in the electrolyte increased.

SUMMARY

AC impedance techniques were used to study the corrosion of 19 alloys under conditions similar to the STS launch environment which is highly corrosive. The 19 alloys were: Zirconium 702, Hastelloy C-22, Inconel 625, Hastelloy C-276, Hastelloy C-4, Inconel 600, 7Mo + N, Ferralium 255, Inco Alloy G-3, 20Cb-3, SS 904L, Inconel 825, SS 304LN, SS 316L, SS 317L, ES 2205, SS 304L, Hastelloy B-2, and Monel 400. AC impedance data were acquired for each of the alloys after one hour immersion in each of the following three electrolytes: 3.55% NaCl, 3.55% NaCl-0.1N HCl, and 3.55% NaCl-1.0N HCl.

The data were analyzed qualitatively by using the Nyquist plot and quantitatively by using the Bode plot. Rp values were obtained from the Bode plot. The corrosion resistance for 17 of the 19 alloys decreased as the concentration of hydrochloric acid in the electrolyte increased. The corrosion resistance of Zirconium 702 and Ferralium 255 increased as the concentration of hydrochloric acid in the electrolyte increased. The most corrosion resistant alloy in the three electrolytes was Zirconium 702. The ordering of the alloys in terms of their resistance to corrosion was different in the three electrolytes.

A good correlation was found between the ac impedance data and the dc polarization data even though the Rp values were different. It is postulated that the Rp values obtained by using ac impedance techniques are more accurate. A comparison with the beach corrosion data led to the conclusion that there is, in general, a good correlation between the materials that performed well in both tests as well as between those that performed poorly. However, the ordering of the materials according to their resistance to corrosion was different in both tests. It can be concluded that ac impedance techniques can be used to choose what materials should be subjected to long-term corrosion testing.

TABLE OF CONTENTS

LIST OF FIGURES

STUDY OF METAL CORROSION USING AC IMPEDANCE TECHNIQUES IN THE STS LAUNCH ENVIRONMENT

I. INTRODUCTION

Flexible metal hoses are used in various supply lines that service the Orbiter at the launch pad. These convoluted flexible hoses were originally constructed of 304L stainless steel. The severely corrosive environment at the launch site caused pitting corrosion in many of these flex hose lines. In the case of vacuum jacketed cryogenic lines, failure of the flex hose by pitting causes a loss of vacuum and subsequent loss of insulation.

The corrosive environment at the launch site is due to the very high chloride content caused by the proximity of the ocean and to the generation of seventeen tons of concentrated hydrochloric acid as a fuel combustion product of the Solid Rocket Boosters during a launch. These corrosive conditions cause severe pitting on some of the commonly used steel alloys.

A previous investigation was undertaken in order to evaluate 19 metal alloys with the purpose of finding a more corrosion resistant replacement material for 304L stainless steel. The tests performed in that investigation were: electrochemical corrosion testing, accelerated corrosion testing in a salt fog chamber, long term exposure at the beach corrosion testing site, and pitting corrosion tests in ferric chloride solution. These tests led to the conclusion that the most corrosion resistant alloys were, in descending order, Hastelloy C-22, Inconel 625, Hastelloy C-276, Hastelloy C-4, and Inco Alloy G-3. Of these top five alloys, the Hastelloy C-22 stood out as being the best of the alloys tested. The details of this investigation are found in report MTB-325-87A (1). Furthermore, on the basis of corrosion resistance combined with weld and mechanical properties, Hastelloy C-22 was determined to be the best material for the construction of flex hoses to be used in fuel lines servicing the Orbiter at the launch site.

The electrochemical corrosion testing done previously was based on the use of dc polarization techniques. In the present investigation, ac impedance techniques will be used in order to study the corrosion of the 19 alloys under three different electrolyte conditions: neutral 3.55% NaCl, 3.55% NaCl-0.1N HCl, and 3.55% NaCl-1.0N HCl. The 3.55% NaCl-0.1N HCl electrolyte provides an environment for the corrosion of the alloys similar to the conditions at the launch pad.

II. MATERIALS AND EQUIPMENT

2.1 CANDIDATE ALLOYS

The nineteen alloys tested and their nominal compositions in weight percent are shown in Table 1. The choice of these alloys for the previous investigation was based on their reported resistance to corrosion.

2.2 AC IMPEDANCE MEASUREMENTS

A model 378 Electrochemical Impedance system manufactured by EG&G Princeton Applied Research Corporation was used for all electrochemical impedance measurements. The system includes: (1) the Model 273 Computer-Controlled Potentiostat/ Galvanostat, (2) the Model 5301A Computer-Controlled Lock-In Amplifier, (3) the IBM XT Microcomputer with peripherals, and the Model 378 Electrochemical Impedance Software.

Specimens were flat coupons 1.59 cm (5/8") in diameter. The specimen holder in the electrochemical cell is designed such that the exposed metal surface area is 1 cm^2.

The electrochemical cell included a saturated calomel reference electrode (SCE), 2 graphite rod counter electrodes, the metal working electrode, and a bubbler/vent tube. Each alloy was studied under three different electrolyte conditions: aerated 3.55% neutral NaCl, aerated 3.55% NaCl-0.1N HCl (similar to the conditions at the launch site), and aerated 3.55% NaCl-1.0N HCl (more aggressive than the conditions at the launch site). All solutions were prepared using deionized water.

III. PROCEDURE FOR AC IMPEDANCE MEASUREMENTS

The test specimens were polished with 600-grit paper, wiped with methyl-ethyl ketone, ultrasonically degreased for five minutes in a detergent solution, rinsed with deionized water, and dried. Each specimen was observed under the microscope and weighed before and after each experiment to monitor changes caused by corrosion on its appearance and weight.

The electrolyte solution was aerated for at least 15 minutes before immersion of the test specimen. Aeration continued throughout the test.

AC impedance measurements were performed under each of the three electrolyte conditions chosen. After immersion in the electrolyte, the sample was allowed to equilibrate for 3600 seconds before the instrument started acquiring data. It was determined previously that after 3600 seconds, the corrosion potential had usually stabilized (2).

AC impedance measurements were gathered in the frequency range from 100 kHz to 0.1001 Hz. A combination of two methods was employed to obtain the data over this wide range of frequencies: (1) phase-sensitive lock-in detection for measurements from 5 Hz to 100 kHz, and (2) the FFT (fast Fourier transform) technique for measurements from 0.1001 Hz to 11 Hz. The data from lock-in (single-sine) and FFT (multi-sine) were automatically merged by the IBM XT microcomputer dedicated software.

The conditions for the lock-in experiments were: initial frequency, 100 kHz; final frequency, 5 Hz; points/decade, 5; AC amplitude, 5 mV; DC potential, 0 vs OC (open circuit); condition time, 0 seconds; condition potential, 0 V; open circuit delay, 3600 seconds. The open circuit potential was monitored with a voltmeter.

The conditions for the FFT experiments were: base frequency, 0.1001 Hz; data cycles, 5; AC amplitude, 10 mV; DC potential, 0 vs OC; open circuit delay, 0 seconds. The open circuit potential was monitored with a voltmeter.

The data for each experiment were plotted in the Nyquist and Bode plot format.

IV. RESULTS AND DISCUSSION

4.1 THEORETICAL BACKGROUND

AC impedance techniques offer some distinct advantages over dc techniques (3). First, the small excitation amplitudes that are used, generally in the ranges of 5 to 10 mV peak-to-peak, cause only minimal perturbations of the electrochemical system, thus reducing errors caused by the measuring technique itself. Second, the technique offers valuable information about the mechanisms and kinetics of electrochemical processes such as corrosion. Third, measurements can be made in low conductivity solutions where dc techniques are subject to serious potential-control errors.

Despite the advantages of the ac impedance techniques mentioned above, their application requires sophisticated techniques in order to interpret the data and extract meaningful results. The application of ac impedance measurements to study corrosion has so far resulted in the publication of a large amount of experimental data without much interpretation. The technique is at the present time in a transition from the data collection stage to the data analysis stage (4).

AC impedance measurements are based on the fact that an electrochemical system, such as those studied in this investigation, can be represented by an equivalent electrical circuit. The equivalent circuit for a simple electrochemical cell is shown in Figure 1 (5). The circuit elements R_{Ω}, Rp, and Cdl represent the uncompensated resistance (resistance from the reference to the working electrode), the polarization resistance (resistance to electrochemical oxidation), and the capacitance very close to the metal surface (at the double layer). There are several formats that can be used for the graphical representation of the ac impedance data (3,6,7). Each format offers specific advantages for revealing certain characteristics of a given test system. It was determined at the beginning of this research, that the most suitable formats for plotting the ac impedance data were the Nyquist and the Bode plots.

The Nyquist plot is also known as a Cole-Cole plot or a complex impedance plane diagram. Figure 2 (5) shows the Nyquist plot for the equivalent circuit shown in Figure 1. The imaginary component of the impedance (Z") is plotted versus the real component of the impedance (Z') for each excitation frequency. As indicated in Figure 2, this plot can be used to calculate the values of R_{Ω}, Rp, and Cdl.

The Bode plot for the equivalent circuit in Figure 1 is shown in Figure 3 (5). This graphical representation of the ac impedance data involves plotting both the phase angle (θ) and

the log of absolute impedance (log|Z|) versus the log of the frequency ($w = 2\pi f$). As indicated on the figure, values for R_Ω, Rp, and Cdl can also be obtained from the Bode plot. Of special interest for this research is the determination of the Rp values which can be used to calculate the corrosion rate of an electrode material in a given electrolyte (3,8).

4.2 RESULTS AND DISCUSSION

The Bode plots included in this report appear in the form of two separate graphs: log|Z| versus log Frequency (Hz) and θ versus log Frequency (Hz). Nyquist (at the top) and Bode (at the bottom) plots for the 19 alloys used in this investigation are shown in Figures 4-13. None of the Nyquist plots obtained in this investigation exhibited the ideal semicircle shown in Figure 2. Experimentally, it has been observed that deviations from the results expected for simple equivalent circuits occur for real, corroding systems (6,9). Some of the deviations that have been observed for real systems are: a semicircle with its center depressed below the real axis, a partial semicircle, and a partial semicircle that changes shape at the low frequency end. Impedance data that result in a Nyquist plot in the form of a depressed or partial semicircle can still be used to calculate Rp values. Several authors have described computer modeling of electrochemical impedance (10,11). The usual approach is to curve-fit the semicircle that results from a single time constant capacitive response. This approach allows an estimate to be made of the low frequency intersection of the semicircle response with the real axis. This procedure is especially important when the response still has a large imaginary contribution at low frequency resulting in a partial semicircle. Deviations that result in a Nyquist plot with the shape of a partial semicircle that changes at the low frequency end require a more complex computer program which contains more circuit elements. The time limitations of this research prevented the use of the methods just mentioned to analyze the Nyquist plots for the 19 alloys.

Valuable qualitative information can be extracted by comparing the Nyquist plots shown in Figures 4-13. Each Figure shows the change in the Nyquist plot for a one hour immersion time of the alloy in the three different electrolytes: (X) 3.55% NaCl, (□) 3.55% NaCl-0.1N HCl and (o) 3.55% NaCl-1.0N HCl. The change in the corrosion rate, which is inversely proportional to Rp, can be estimated qualitatively by looking at the change in the Nyquist plot. Zirconium 702 (Figure 4a) stands out as being the most corrosion resistant alloy under the conditions used in this study. Its Rp was not only the highest but it also showed the least change upon increasing the concentration of the hydrochloric acid from 0.0N to 0.1N to 1.0N; that is, Zirconium 702 became more corrosion resistant as the concentration of hydrochloric acid increased. This finding

agrees with the known fact that Zirconium is resistant to hydrochloric acid at all concentrations up to boiling temperatures. However, there are indications that the metal is vulnerable to pitting in seawater (12). Ferralium 255 (Figure 4b) also became more corrosion resistant upon increasing the concentration of the acid. Its Rp values were similar in the three electrolytes but lower than those for Zirconium 702. The change in Rp for the other 17 alloys upon increasing the concentration of the acid in the electrolyte was in the opposite direction to that observed for Zirconium 702 and Ferralium 255; they became less resistant to corrosion as the concentration of the acid increased. Hastelloy C-22 (Figure 5a), Inco Alloy G-3 (Figure 5b), Hastelloy C-4 (Figure 6a), Inconel 625 (Figure 6b), Hastelloy C-276 (Figure 7a), and Hastelloy B-2 (Figure 7b) have similar Nyquist plots showing the decrease in Rp as the concentration of the acid increases. The decrease in Rp appears as an increase in the curvature of the partial semicircle. Monel 400 (Figure 8a) shows partial semicircles with a slight decrease in Rp caused by increasing the acid concentration. The semicircle obtained in 3.55% NaCl-0.1N HCl has a feature at the end (a straight line with a positive slope) that has been associated with a Warburg impedance (13). This behavior has been explained by postulating an extra impedance term in the equivalent circuit that is associated with diffusion controlled processes. 20Cb-3, ES 2205, and 7Mo + N (Figures 8b, 9a, 9b) show similar changes in the Nyquist plot. No drastic change in the Rp values is observed when the concentration of hydrochloric acid increases from 0.0N to 0.1N (as indicated by the two parallel lines in the Nyquist plot). However, there is a significant change in the Nyquist plot when the concentration of the acid is increased to 1.0N that results in a considerable decrease in Rp. The turn at the low frequency end of the curve is probably an indication of a diffusion process taking place. SS 304L (Figure 10a) shows a Nyquist plot that is different from all the others. It should be pointed out that one of the experiments involving SS 304L resulted in the partial breakdown of the surface of the metal sample. Data from that experiment were discarded. The complex Nyquist plot obtained for SS 304L in 3.55% NaCl-1.0N HCl is similar to the Nyquist plot obtained for a pin-holed coal tar epoxy coating on mild steel (13). SS 304LN (Figure 10b) showed good resistance to corrosion in neutral 3.55% NaCl but similar low resistance to corrosion (low Rp values) in 3.55% NaCl-0.1N HCl and 3.55% NaCl-1.0N HCl. Inconel 600 (Figure 11a) showed a similar behavior. Inconel 825, SS 317L, SS 904L, and SS 316L (Figures 11b, 12a, 12b, 13a) show a similar behavior indicating comparable resistance to corrosion in 3.55% NaCl and 3.55% NaCl-0.1N HCl and a considerably lower resistance to corrosion in 3.55% NaCl-1.0N HCl.

Since the Nyquist plots obtained in this investigation did not resemble the ideal Nyquist plot shown in Figure 2,

calculation of Rp values from those plots was not pursued. It was decided that the Bode plot is a more straightforward means of presenting the data in order to calculate Rp. In a Bode plot, the impedance of a "perfect capacitance" can be represented as a straight line with a slope of -1 and a phase angle of -90°. A "resistor" will plot as a horizontal line for the log|Z| with a phase angle of 0°. A Warburg impedance is a straight line with a slope of -1/2 and a phase angle of -45° (14). The data gathered for the 19 alloys, when plotted in the Bode format (lower plot in Figures 4-13) were interpreted as shown in Figure 3. The value of Z at the lowest frequency (0.1001 Hz) is the sum of Rp and R while the value of Z at the highest frequency (100.020 kHz) is R . The values for Rp obtained from the Bode plot data after one hour immersion in the three different electrolytes are given in Table 2. These values indicate that Zirconium 702 is the most corrosion resistant alloy under the conditions used in this study. The ranking of the other 18 alloys differs for the three electrolytes. In general, it can be concluded that for all the alloys, with the exception of Zirconium 702 and Ferralium 255, the Rp values decrease as the concentration of hydrochloric acid increases in the electrolyte. The changes in Rp can thus be followed qualitatively by examining the data in the Nyquist plot format and quantitatively by using the Bode plot format.

4.3 COMPARISON WITH DC POLARIZATION RESULTS

A comparison of the Rp values obtained in this investigation with the Rp values obtained by dc polarization techniques for the same alloys in 3.55% NaCl-0.1N HCl (ref. 2, Table 3) and for 10 of the alloys in 3.55% NaCl-1.0N HCl (ref. 2, Table 9), indicates that there is no correlation between the actual values of Rp. However, there is a good correlation between the ordering of the alloys according to their resistance to corrosion by both methods even though the ordering does not match exactly. The fact that ac impedance techniques use only very small signals which do not disturb the electrode properties to be measured can be used to support the validity of the Rp values obtained by this technique.

4.4 COMPARISON WITH BEACH CORROSION DATA

A comparison of the Rp values obtained from ac impedance measurements with the beach corrosion data for all the alloys in 3.55% NaCl-1.0N HCl (ref. 2, Figure 9) indicates that there is, in general, a good correlation even though the ranking of the metals does not match exactly. For example, Hastelloy C-22 was the most resistant alloy when tested at the beach corrosion site while it ranked seventh according to the Rp value in this study. It should be pointed out that, as a group, there is a good correlation between the alloys that performed at the top (Zirconium 702, Ferralium 255, Inconel 625, Inco Alloy G-3, Hastelloy C-4, Hastelloy, C-276, and

Hastelloy C-22) in both investigations. A tentative conclusion that can be drawn from this comparison is that the ac impedance technique can be used to choose what materials should be subjected to long-term corrosion testing at the beach testing site. The lack of a close correlation between the ac impedance data and the beach corrosion data may result from the fact that the ac impedance measurements were obtained for the alloys after one hour immersion in the aerated electrolytes at room temperature. The conditions at the beach testing site are obviously different (ref. 1, p. 8) and more similar to the conditions in the STS launch environment. The results from the present investigation may be more appropriate for testing the corrosion resistance of alloys that are going to be in contact with liquid electrolytes such as the ones used here.

V. CONCLUSIONS

1. AC impedance techniques, when used for corrosion testing, provide useful qualitative (Nyquist plot) and quantitative information (Rp values) that can be used to screen alloys to be subjected to long-term corrosion testing.

2. The Rp values obtained for the 19 alloys under three different electrolyte conditions can be used to rank the alloys according to their resistance to corrosion since Rp is inversely proportional to the rate of corrosion.

3. Zirconium 702 was found to be the most corrosion resistant alloy under the conditions used in this investigation.

4. There is a good general agreement between the results obtained using dc and ac techniques even though the actual Rp values were found to be different. It is postulated that the Rp values obtained by the ac technique are more accurate.

VI. FUTURE WORK

1. AC impedance measurements involving longer immersion times to investigate how the Rp value -and therefore the rate of corrosion- changes with time.

2. Implementation of the use of software to perform the analysis of the data in the Nyquist plot format in order to calculate Rp values.

3. Include testing of alloys after exposure to conditions as similar to the STS launch environment as possible.

4. Study the effect of protective coatings on the rate of corrosion of the 19 alloys.

5. Modify the electrolyte conditions to include other chemicals normally found at the STS launch environment.

6. Study the effect that a change in temperature, similar to the seasonal changes that occur at the STS launch environment, would have on the rate of corrosion.

REFERENCES

1. MacDowell, L.G. and Ontiveros, C., Evaluation of Candidate Alloys for the Construction of Metal Flex Hoses in the STS Launch Environment, Test Report, Document No. MTB-325-87A, National Aeronautics and Space Administration, Kennedy Space Center, Materials Testing Branch, August 23, 1988.

2. Ontiveros, C., Localized Corrosion of Candidate Alloys for Construction of Flex Hoses, 1987 NASA/ASEE Summer Faculty Fellowship Program Research Reports, Kennedy Space Center, 1987.

3. Application Note AC-1, Basics of AC Impedance Measurements, EG&G PARC, Princeton, NJ., 1984.

4. Mansfeld, F., Don't Be Afraid of Electrochemical Techniques -But Use Them with Care!, Corrosion, Vol. 44, pp. 856-868, 1988.

5. Rothstein, M.L., Electrochemical Corrosion Measurements for the Metal Finishing Industry, Application Note Corr-5, EG&G PARC, Princeton, NJ., 1986.

6. Mansfeld, F., Recording and Analysis of AC Impedance Data for Corrosion Studies. I. Background and Methods of Analysis, Corrosion, Vol. 37, pp. 301-307, 1981.

7. Mansfeld, F., Kendig, M.W., and Tsai, S., Recording and Analysis of AC Impedance Data for Corrosion Studies. II. Experimental Approach and Results, Vol. 38, pp. 570-580, 1982.

8. Lorenz, W.J. and Mansfeld, F., Determination of Corrosion Rates by Electrochemical DC and AC Methods, Corrosion Science, Vol. 21, pp. 647-672, 1981.

9. Williams, D.E. and Naish, C.C., An Introduction to the AC Impedance Technique, and its Application to Corrosion Problems, U.K. Atomic Energy Authority, Harwell Report AERE-M3461, pp. 1-10, 1985.

10. Moody, J.R., Quin, X.P., and Strutt, J.E., The Application of a Compurerized impedance Monitoring System to a Study of the Behavior of 347 ss in Nitric Acid, presented at the 166th Meeting of the Electrochemical Society, New Orleans, Louisiana, 1984.

11. Kendig, M.W., Meyer, E.M., Lindberg, G. and Mansfeld, F., A Computer Analysis of Electrochemical Impedance Data, Corrosion Science, Vol. 23, pp. 1007-1015, 1983.

12. Uhlig, H.H., Corrosion and Corrosion Control. An

Introduction to corrosion science and engineering, Second Edition, John Wiley & Sons Inc., p. 368, 1971.

13. Scantlebury, J.D., Ho, K.N. and Eden, D.A., Impedance Measurements on Organic Coatings on Mild Steel in Sodium Chloride Solutions, Electrochemical Corrosion Testing, ASTM STP 727, Mansfeld, F. and Bertocci, U., Eds., American Society for Testing and Materials, pp. 187-197, 1981.

14. Cahan, B.D. and Chien, C., The Nature of the Passive Film of Iron. II. A-C Impedance Studies, J. Electrochem. Soc., Vol. 129, pp. 474-480, 1982.

TABLE 1 CANDIDATE ALLOYS AND THEIR NOMINAL COMPOSITIONS (WT%)

ALLOY	Ni	Fe	Cr	Mo	Mn*	Co*	Cu	C*	Si*	P*	S*	Other
HASTELLOY C-4	Bal.	3.0	16	17	1.0	2.0		0.01	0.08	0.02	0.01	Ti 0.7
HASTELLOY C-22	Bal.	3.0	22	13	0.5	2.5		0.01	0.08	0.02	0.01	V 0.3, W 3
HASTELLOY C-276	Bal.	7.0	17	17	1.0	2.5		0.01	0.08	0.02	0.01	V 0.3, W 4.5
HASTELLOY B-2	Bal.	2.0	1	28	1.0	1.0		0.01	0.1	0.02	0.01	
INCONEL 600	Bal.	8.0	16		1.0		0.5	0.15	0.5		0.01	
INCONEL 625	Bal.	5.0	23	10	0.5	1.0		0.10	0.5	0.01	0.01	Cb 4.1
INCONEL 825	Bal.	22.0	21	3	1.0		2.5	0.05	0.5		0.03	
INCO G-3	Bal.	20.0	22	7	1.0	5.0	2.0	0.02	1.0	0.04	0.03	Cb 0.5, W 1.5
MONEL 400	Bal.	2.5			2.0		31	0.30	0.5		0.02	
ZIRCONIUM 702												Zr 99.2, Hf 4.5
SS 304L	10	Bal.	19		2.0			0.03	1.0			
SS 304LN	10	Bal.	19		2.0			0.03	1.0	0.04	0.03	N 0.13
SS 316L	12	Bal.	17	2.5	2.0			0.03	1.0	0.04	0.03	
SS 317L	13	Bal.	19	3.5	2.0			0.03	1.0			
SS 904L	25	Bal.	21	4.5	2.0		1.5	0.02	1.0	0.04	0.03	
20 Cb-3	35	Bal.	20	2.5	2.0		3.5	0.07	1.0			
7Mo + N	4	Bal.	28	2	2.0			0.03	0.8	0.03	0.01	N 0.25
ES 2205	5	Bal.	22	3	2.0			0.03	1.0	0.03	0.02	N 0.14
FERRALIUM 255	5	Bal.	26	3	1.5		2.0	0.04	1.0	0.04	0.03	N 0.17

* Values are max.

TABLE 2

POLARIZATION RESISTANCE IN 3.55% NACL

MATERIAL NAME	Rp (ohms)
ZIRCONIUM 702	60884
HASTELLOY C-22	23146
INCONEL 625	18338
HASTELLOY C-276	17121
HASTELLOY C-4	15797
INCONEL 600	15426
7MO + N	15394
FERRALIUM 255	15057
INCO ALLOY G-3	14787
20CB-3	14660
SS 904L	14449
INCONEL 825	14237
SS 304N	13103
SS 316L	12598
SS 317L	12290
ES-2205	11913
SS 304L	11383
HASTELLOY B-2	3779
MONEL 400	652

TABLE 3

POLARIZATION RESISTANCE IN 3.55% NACL-0.1N HCL

MATERIAL NAME	Rp (ohms)
ZIRCONIUM 702	59937
FERRALIUM 255	15675
20CB-3	15369
SS 317L	14745
SS 316L	14290
INCONEL 625	13798
INCONEL 825	13281
ES-2205	13227
SS 904L	12786
INCO ALLOY G-3	12716
7MO + N	12502
HASTELLOY C-4	11723
HASTELLOY C-276	10947
HASTELLOY C-22	9758
HASTELLOY B-2	1806
SS 304L	778
MONEL 400	586
SS 304LN	531
INCONEL 600	498

TABLE 4

POLARIZATION RESISTANCE IN 3.55% NACL-1.0N HCL

MATERIAL NAME	Rp (ohms)
ZIRCONIUM 702	57081
FERRALIUM 255	15133
INCONEL 625	12213
INCO ALLOY G-3	11665
HASTELLOY C-4	8698
HASTELLOY C-276	7201
HASTELLOY C-22	6800
HASTELLOY B-2	1487
MONEL 400	538
INCONEL 825	490
INCONEL 600	481
SS 304LN	431
20CB-3	422
SS 304L	325
SS 904L	300
SS 317L	203
SS 316L	158
ES-2205	101
7MO + N	49

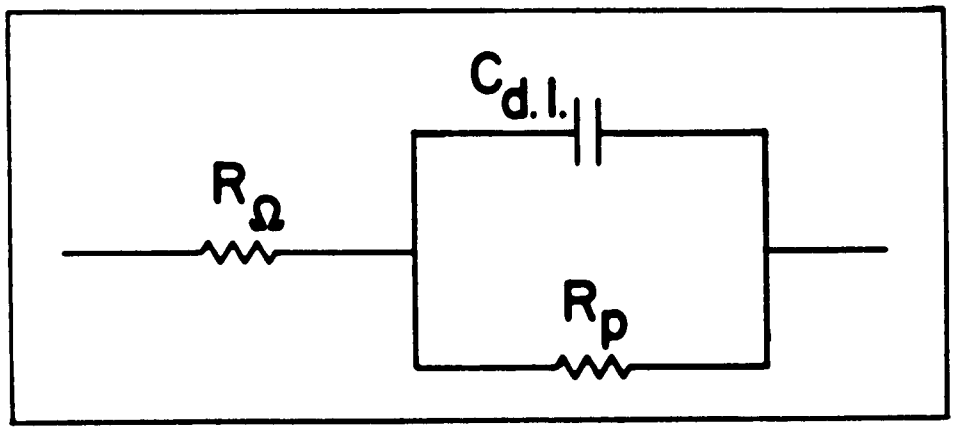

Figure 1. Equivalent circuit for a simple electrochemical cell.

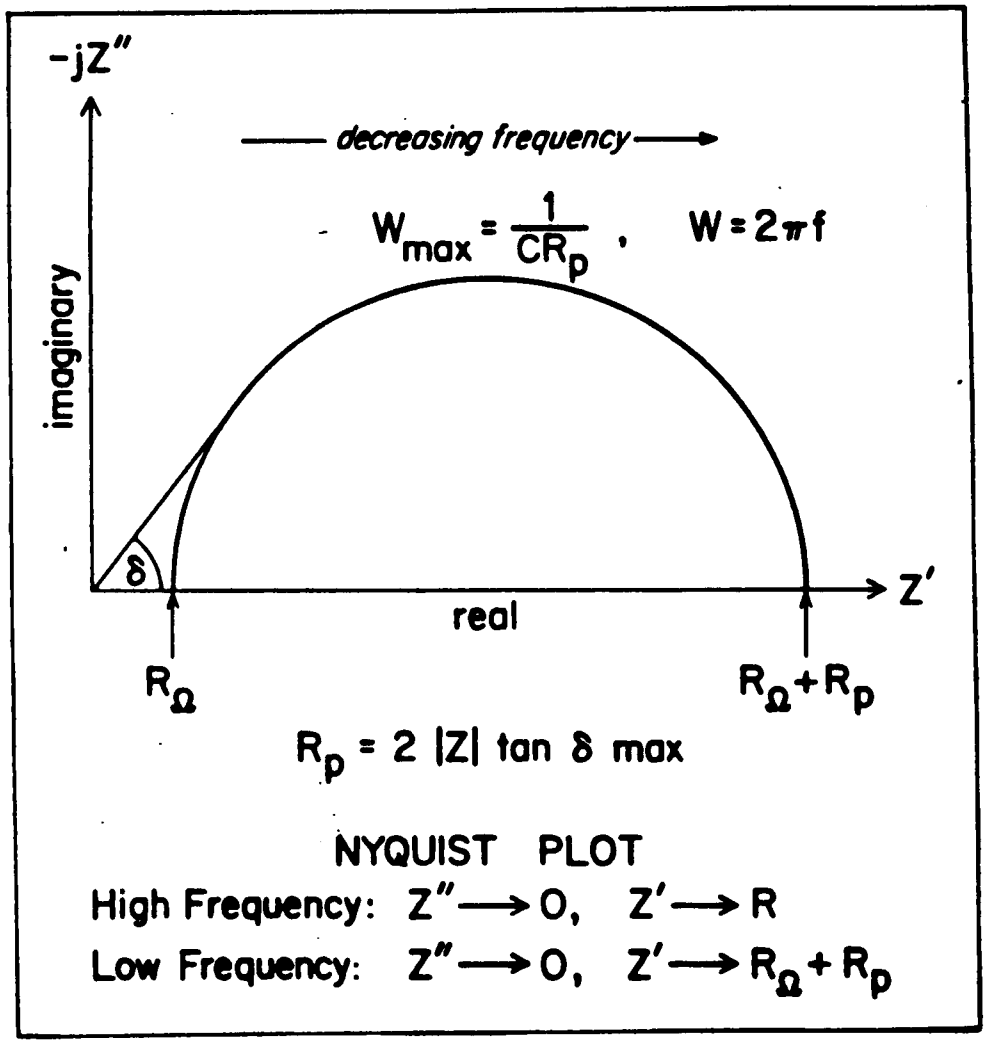

Figure 2. Nyquist plot for equivalent circuit in Figure 1.

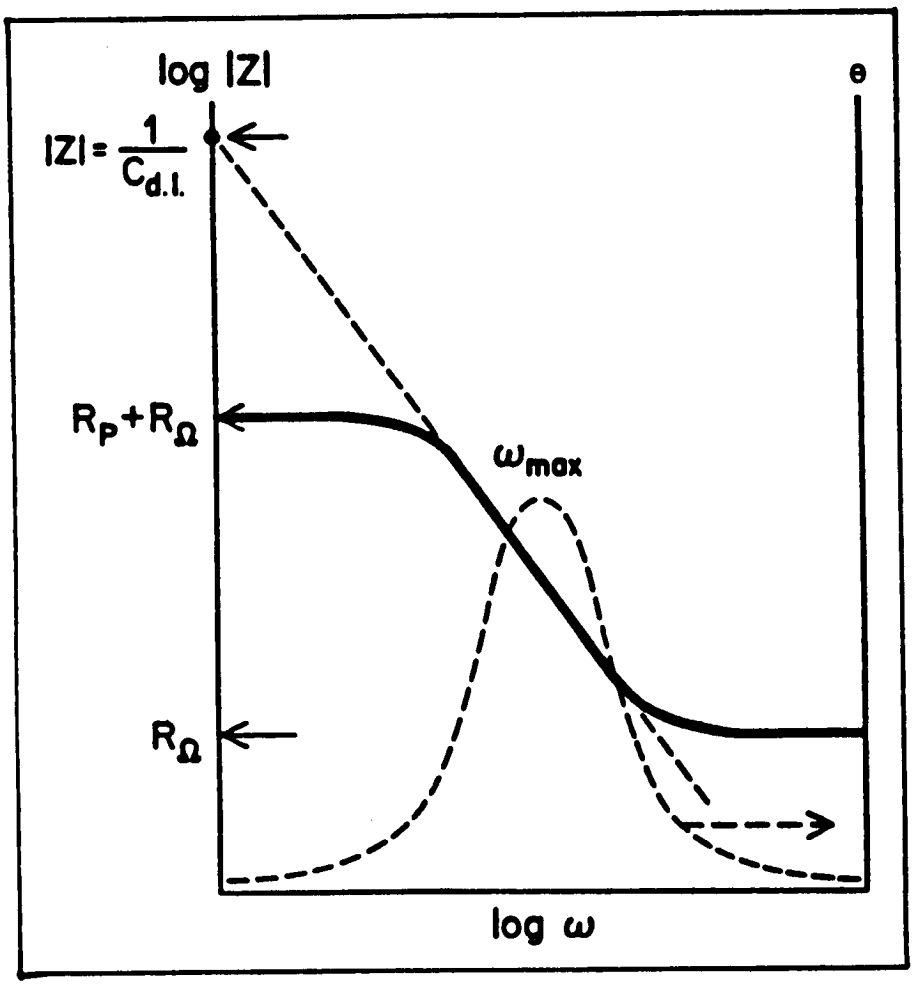

Figure 3. Bode plot for equivalent circuit in Figure 1.

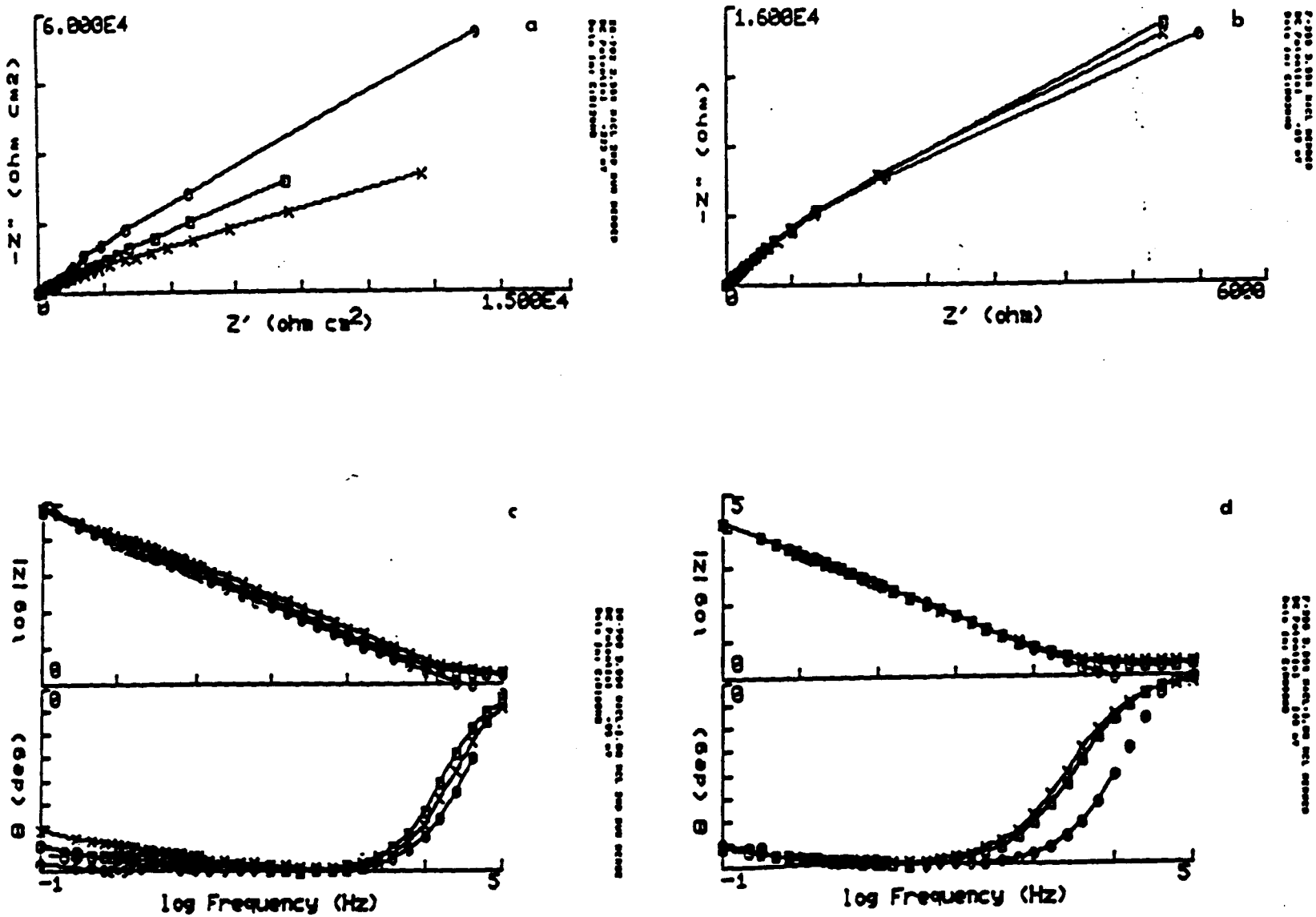

Figure 4. Nyquist and Bode plots for Zirconium 702 (a,c) and Ferralium 255 (b,d).

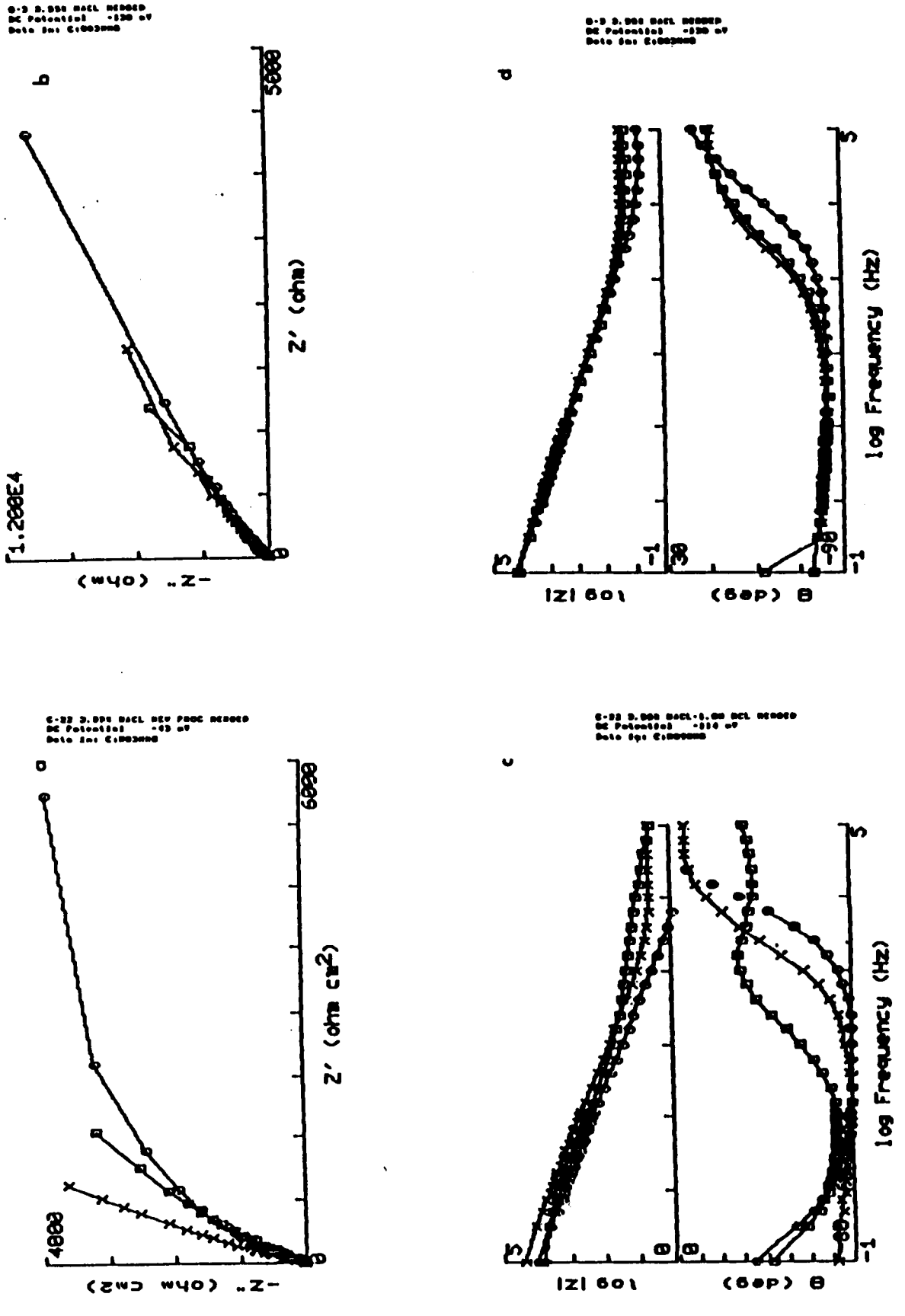

Figure 5. Nyquist and Bode plots for Hastelloy C-22 (a,c) and Inco Alloy G-3 (b,d).

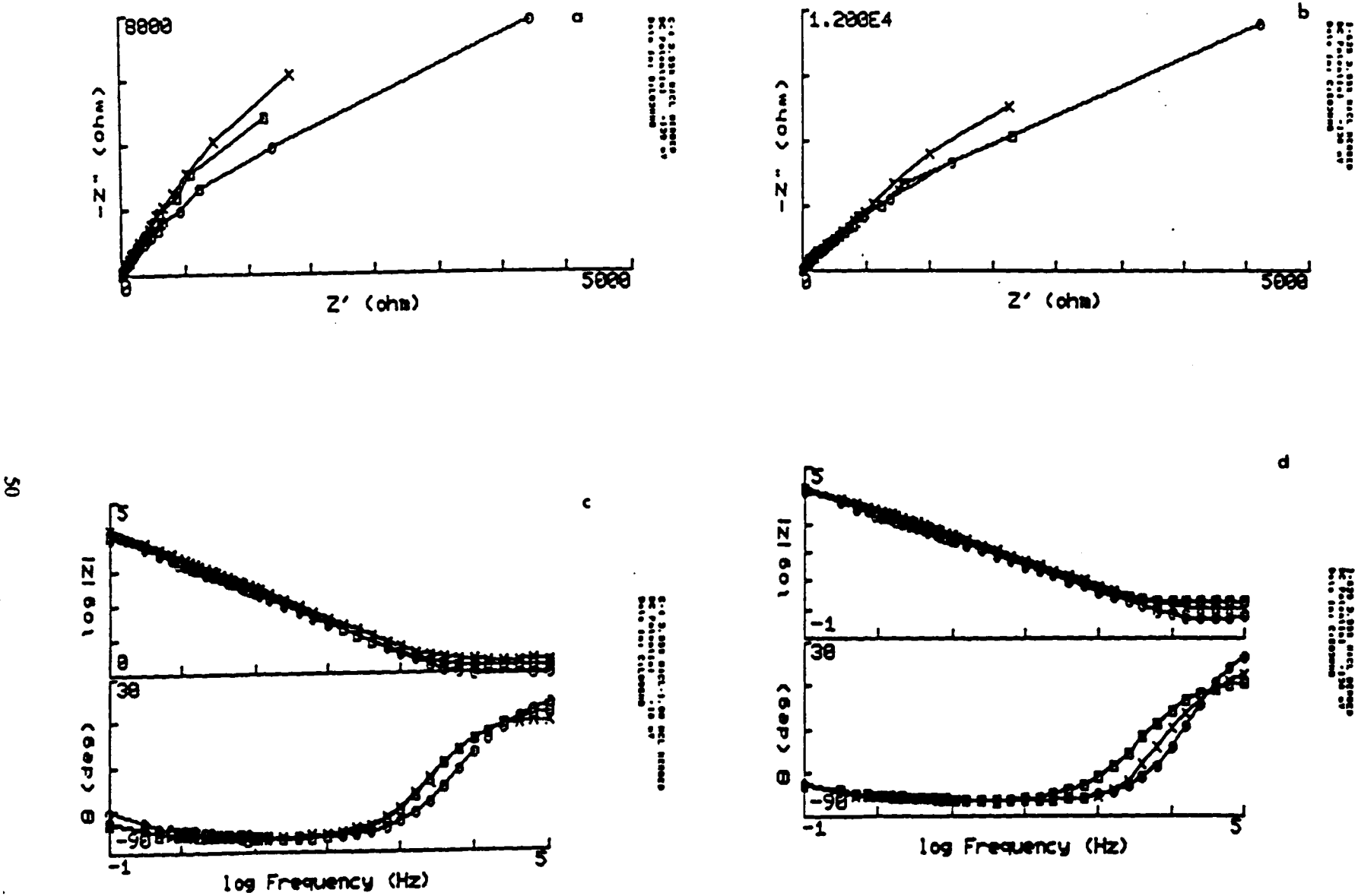

Figure 6. Nyquist and Bode plots for Hastelloy C-4 (a,c) and Inconel 625 (b,d).

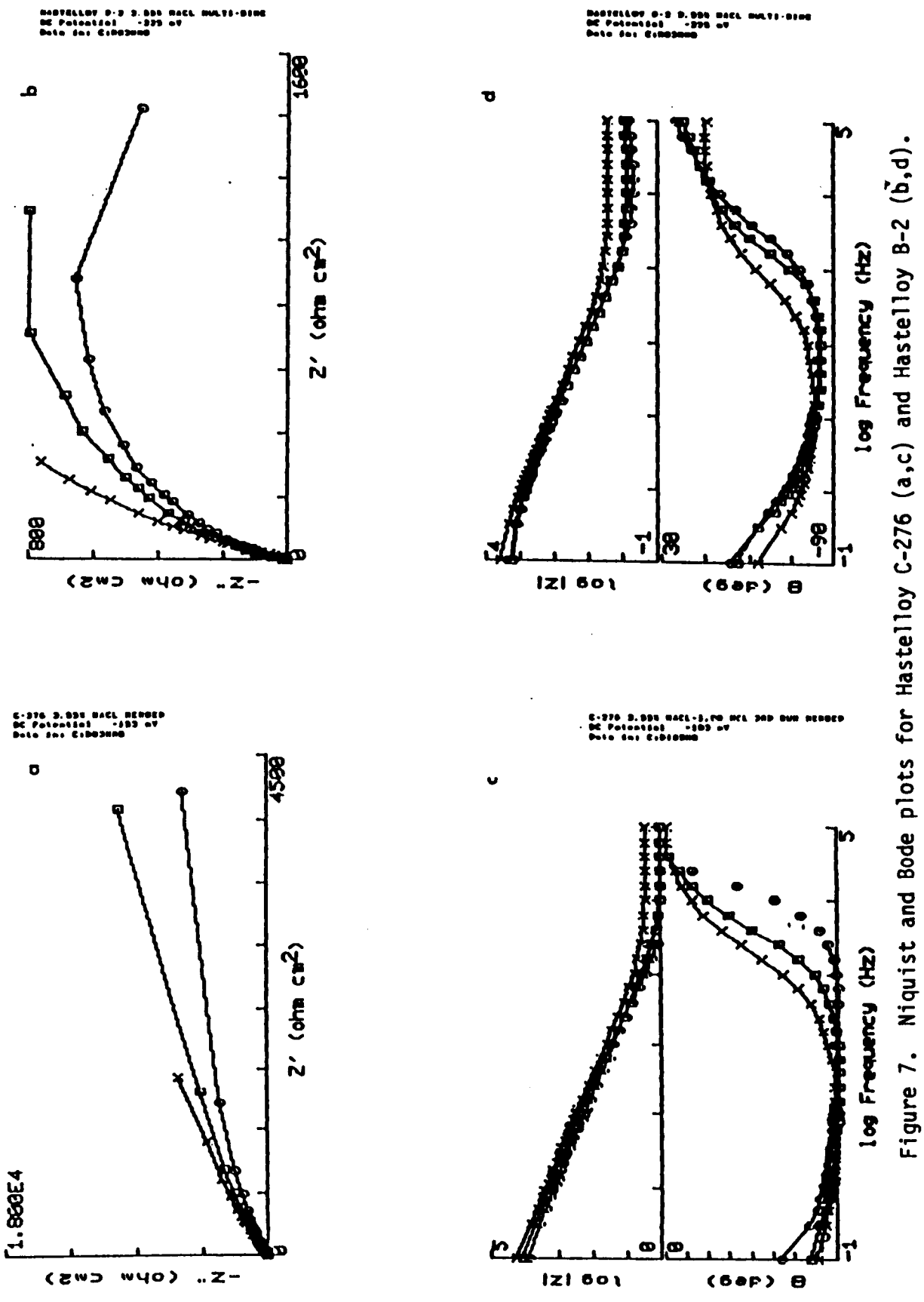

Figure 7. Niquist and Bode plots for Hastelloy C-276 (a,c) and Hastelloy B-2 (b,d).

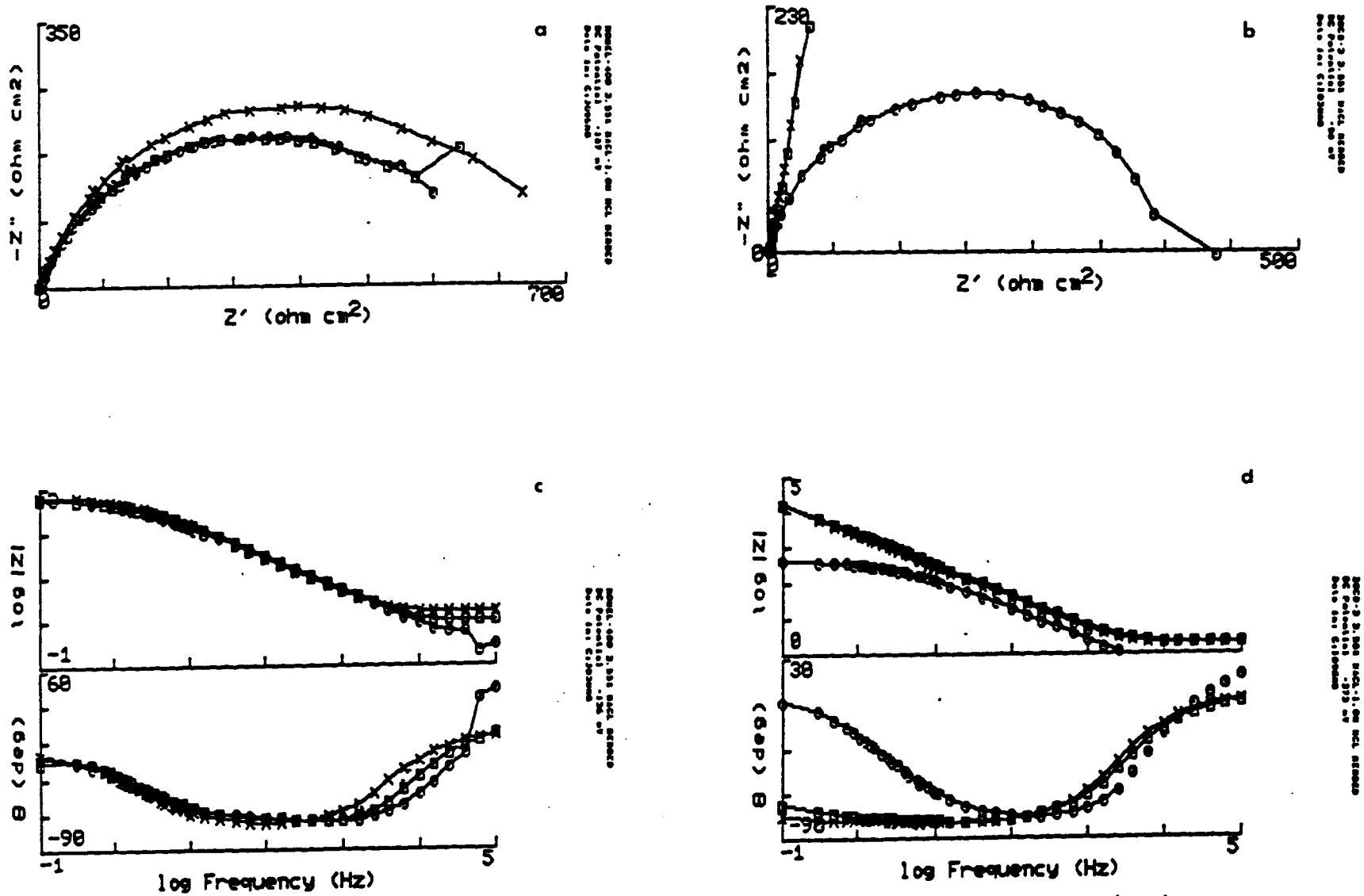

Figure 8. Nyquist and Bode plots for Monel 400 (a,c) and 20Cb-3 (b,d).

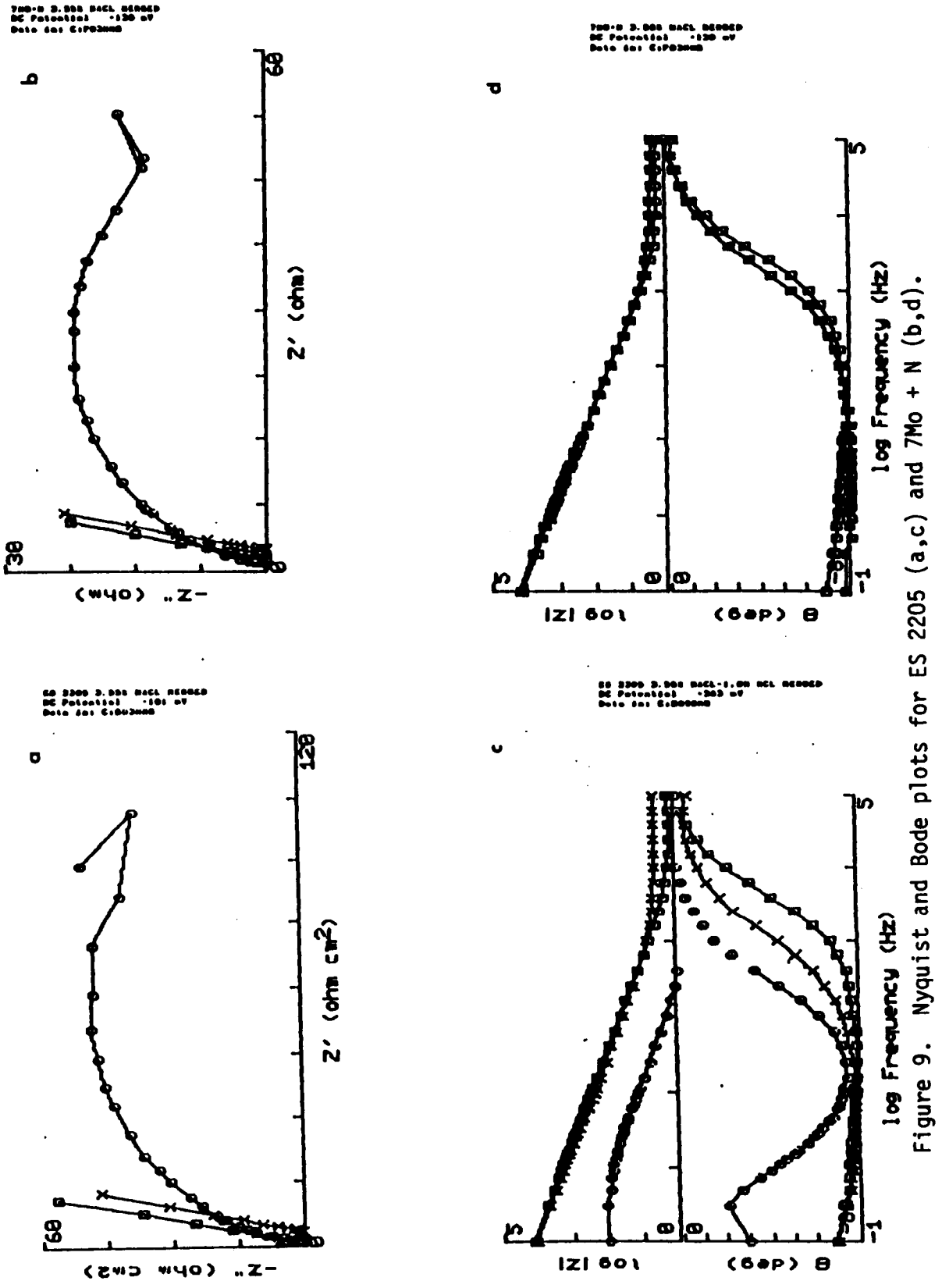

Figure 9. Nyquist and Bode plots for ES 2205 (a,c) and 7Mo + N (b,d).

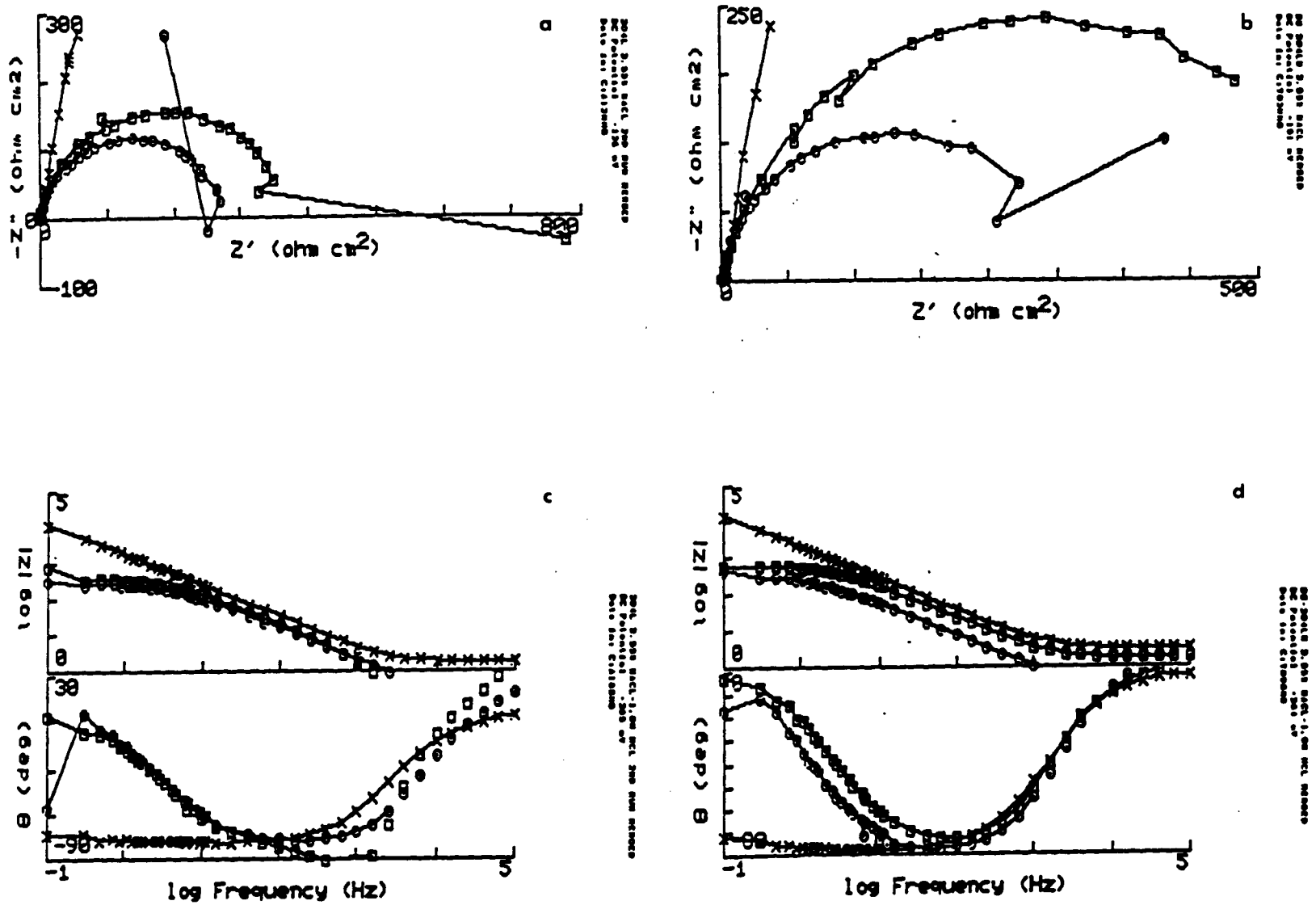

Figure 10. Nyquist and Bode plots for SS 304L (a,c) and SS 304LN (b,d).

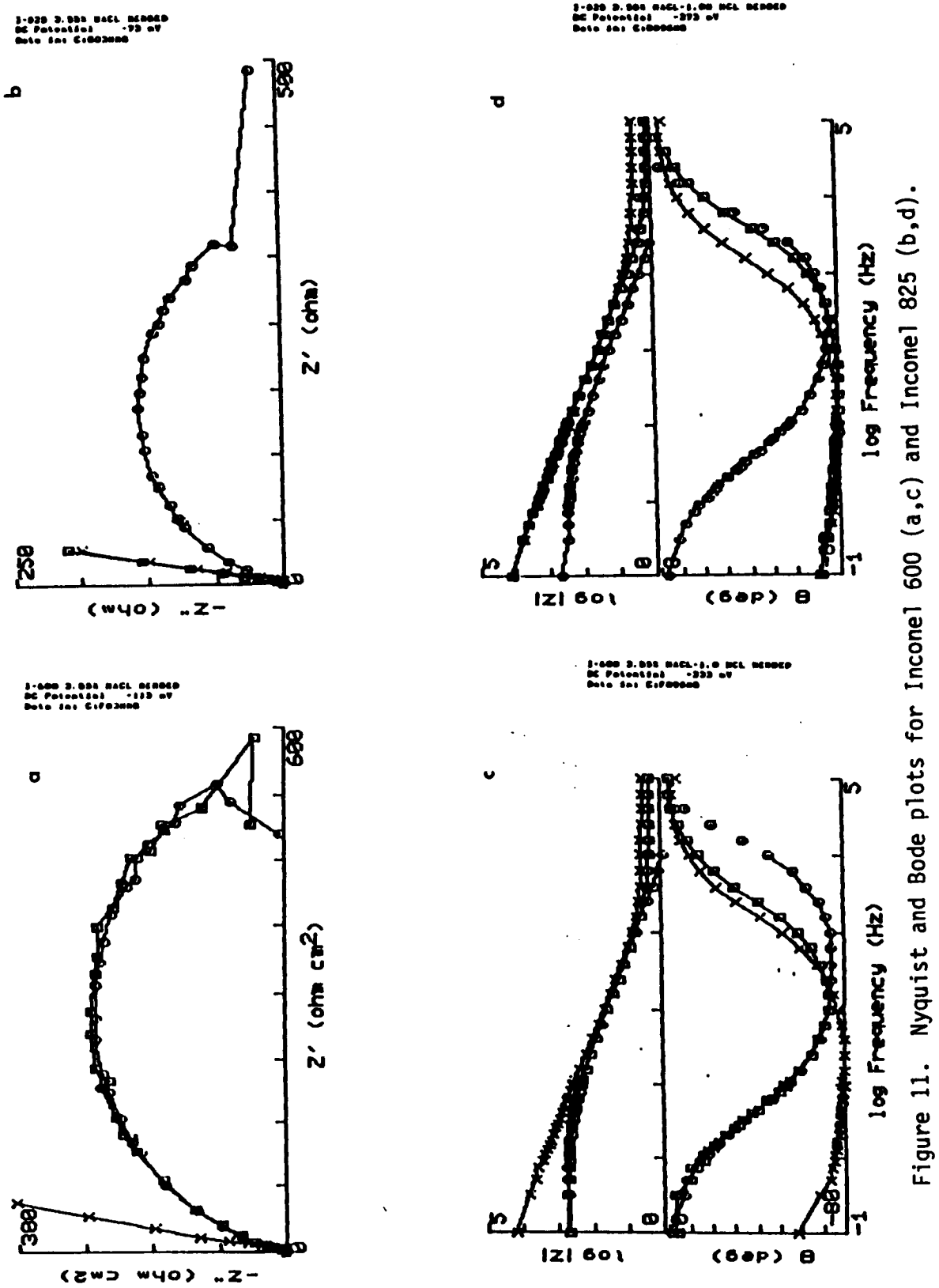

Figure 11. Nyquist and Bode plots for Inconel 600 (a,c) and Inconel 825 (b,d).

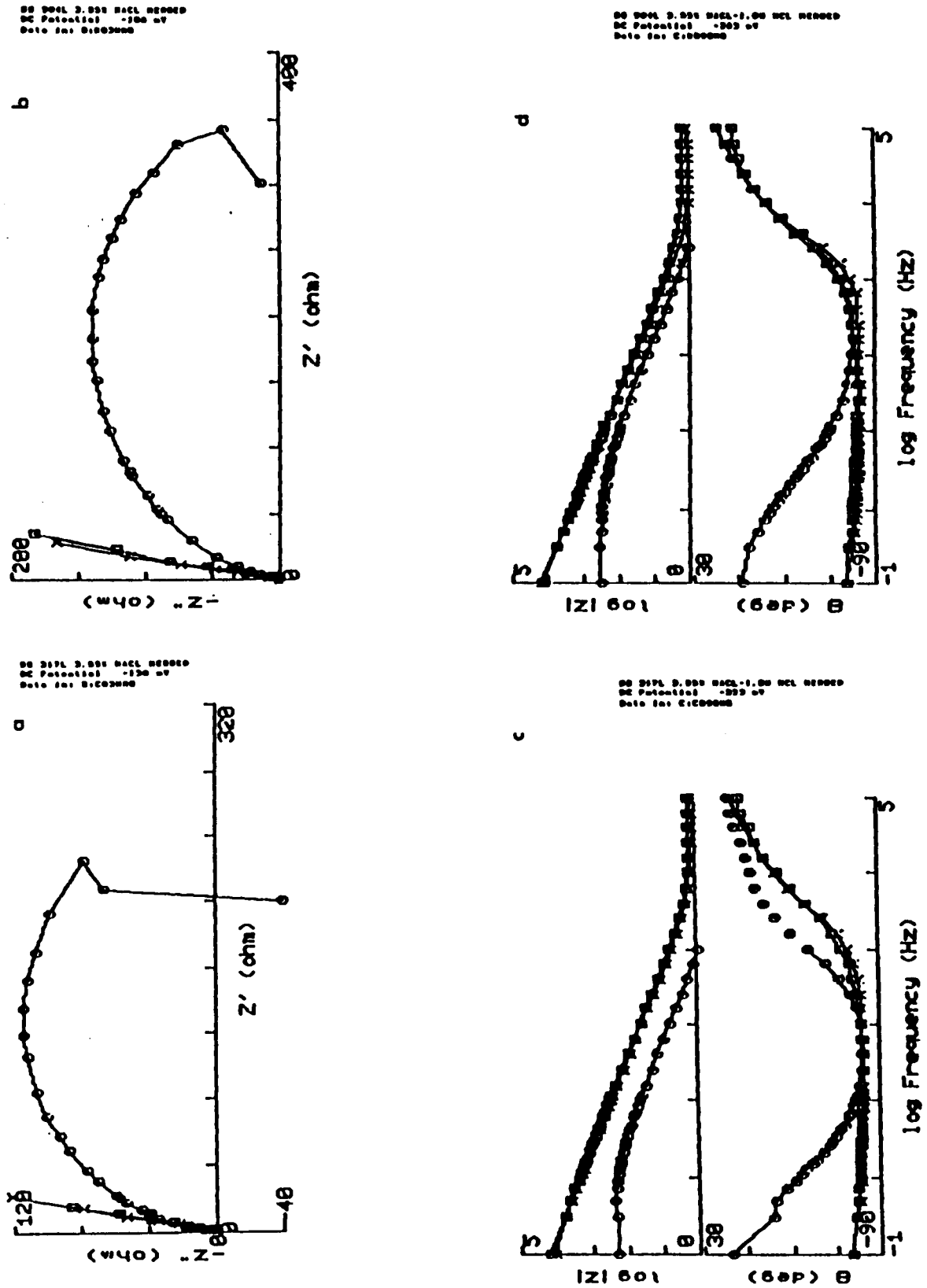

Figure 12. Nyquist and Bode plots for SS 317L (a,c) and SS 904L (b,d).

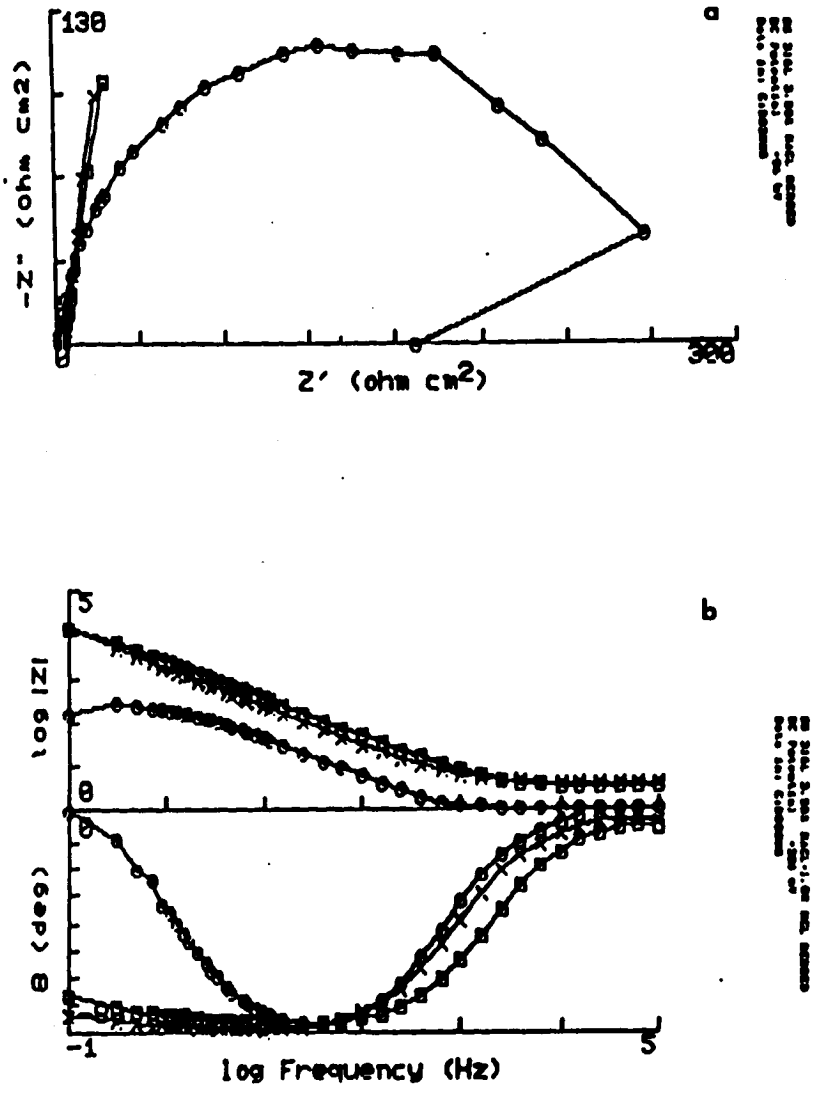

Figure 13. Nyquist and Bode plots for SS 316L (a,b).